Comparison of High Resolution Petrophysical Screening Measurements on Core from a North Sea Jurassic Reservoir

Emmanuel Okwoli, David K. Potter

Department of Physics, University of Alberta

Summary

High resolution, non-destructive screening techniques on slabbed core provide a rapid, cost-effective means of characterizing variations of petrophysical parameters in heterogeneous reservoirs. In this study, we compared results from a large dataset of high resolution probe permeability, probe acoustics and linear X-ray measurements in a heterogeneous North Sea Jurassic reservoir. The purpose was to compare the techniques to predict petrophysical parameters at high resolution.

Conventional core plug analysis has some limitations. It is expensive and time consuming to cut plugs every 1 foot along the core, and the selected plugs might not be representative of the full range of lithologies. For instance, key geologic features such as thin naturally cemented zones may be missed. In contrast, screening techniques have several advantages: they are rapid, non-destructive and allow measurements to be made at high resolution (at the fine lamina scale).

The results of this study showed that there were strong correlations between the different parameters, enabling high resolution measurements of any one of these parameters to predict the high resolution profiles of the other parameters. We also applied backpropagation neural networks (BPNNs) to make predictions using combinations of the different measurements. The different cases we considered produced very good correlations between the measured and predicted parameters with some cases giving perfect correlations with a regression coefficient of determination (R^2 value) of 1.00.

Methodology

Quantitative linear X-ray (probe luminance), probe acoustic and probe permeability measurements were undertaken at high resolution (about every 0.03 feet) in a 36 ft interval of a shoreface Jurassic reservoir in the North Sea. Probe porosity data derived from both the horizontal and vertical acoustic measurements were also analyzed. The main reservoir unit was a quartz sandstone shoreface facies intercalated with clay. This unit was overlain by a 5 ft calcite cemented layer and underlain with a micaceous sandstone. We adopted methods utilizing both parametric and non-parametric regression and multivariate statistical analysis. The non-parametric method involved a Multi-Layer Neural Network (MLNN) utilizing a back propagation (BP) learning algorithm. Different cases were considered for training the predictor. The data was divided into two parts: training data (70 %) and validation data (30 %). Back propagation neural networks (BPNNs) have been popular for predicting petrophysical parameters using a combination of well logs and plug data (Osborne, 1992; Sbiga and Potter, 2017; Zhong et al., 2019). In the present study we wanted to see whether it can be useful for predicting high resolution screening data.

Results

Correlation of the petrophysical parameters

To compare the different petrophysical parameters, we first cross plotted the raw data and observed that the regression correlations were quite low. We then decided to smooth the data by averaging over different vertical intervals (1 ft, 1.5 ft, and 2 ft). This significantly improved the coefficient of determination (R^2) values, with the highest R^2 values obtained when averaging over a 2 ft vertical interval.

The correlation between luminance and probe permeability gave an R^2 value of 0.48 when comparing the raw data, and a much improved R^2 value of 0.76 when the smoothed luminance data was plotted against the smoothed probe permeability values. The reasons will be discussed in the presentation. For the vertical acoustics versus probe permeability an R^2 value of 0.41 was obtained for the raw data, and an R^2 value of 0.85 for the data averaged vertically over 2 ft depth intervals. Likewise, for the vertical acoustics and luminance measurements an initial R^2 value of 0.51 was obtained for the raw data, and a value of 0.70 for the data averaged vertically over 2 ft depth intervals.

Predicting petrophysical parameters using the equations of the regression lines for the smoothed data

Figure 1 (a) shows the luminance predicted permeability using the regression line from the luminance versus permeability crossplot (for the smoothed data averaged over 2 ft vertically) together with the measured probe permeability. Both curves follow the same trend for much of the study interval. There were some small differences, for example between depths of about 7.5 to 14 ft and 16 to 21 ft respectively, possibly due to the presence of the clay intercalated with the sandstone at those depths. The prediction of permeability from vertical acoustic measurements was close to the measured values for the first 30 ft (**Figure 1 (b)**). However, below 30 ft within the micaceous sandstone there was disagreement, with the vertical acoustic measurement predicting higher permeability than was measured. In contrast, the horizontal acoustic measurement gave a better prediction of permeability within the micaceous sandstone interval (**Figure 1 (c)**). A possible reason for the different results seems to be related to the alignment of the mica grains within this anisotropic sandstone.

A summary of the performance evaluation of the predictions based on the regression equations of the different crossplots is given in **Table 1**. Although the coefficient of determination R^2 was quite high for most of the cases considered, the errors were also relatively high for this method of prediction.

Predicting the probe petrophysical parameters using BPNNs

In order to improve the predictions and reduce the relatively high errors associated with the regression method above, we utilized back propagation neural networks using training data based on combinations of the different probe measurements. A summary of the validation results obtained from training the different combinations of probe data is given in **Table 2**, which shows the values of the coefficient of determination (R^2), mean absolute error (MAE), and the root mean squared error (RMSE), between the measured and predicted parameters. The results show very high R^2 values, with cases 3, 4 and 6 giving perfect correlations, and much lower errors than the parametric (regression) method. Thus, the non-parametric method using BPNNs outperformed the parametric method.

Figure 2a shows a crossplot of computed porosity (derived from the horizontal probe acoustic data in conjunction with some calibration porosity measurements) and the neural network predicted porosity trained using all the available smoothed probe data (**Case 4**). The regression coefficient R^2 gave a value of 1.00. **Figure 2b** shows the associated variation with depth of the computed porosity and the neural network predicted porosity trained using all smoothed probe data.

Conclusions

1. This study demonstrates that the probe methods provide a useful alternative to cutting and analyzing core plugs, by allowing rapid, non-destructive, high resolution and inexpensive measurements.

2. The useful correlations between the different high resolution probe screening parameters potentially enables measurements of any one of these parameters to predict the others in this type of reservoir.

3. The non-parametric method, which utilizes the BPNN trained on different combinations of probe measurements, gave a better result with lower error compared with the parametric method.

Table 1: Performance evaluation of the predictions based on the regression equations of the different crossplots for the smoothed data (2 ft vertical averaging).

Crossplotted parameters	Coefficient of determination R^2	Predicted parameters	Mean absolute error (MAE)	Root mean squared error (RMSE)
Luminance and permeability	0.76	Luminance predicted permeability	124.77	270.58
Vertical acoustics and permeability	0.85	Vertical acoustic predicted permeability	110.53	187.42
Horizontal acoustics and permeability	0.37	Horizontal acoustic predicted permeability	69.88	104.93
Vertical acoustics and luminance	0.70	Vertical acoustic predicted luminance	8.10	10.63

Table 2: Summary of the performance of the validation data of the different BPNN cases.

Input parameters	Output	Coefficient of determination (R^2)	Mean absolute error (MAE)	Root mean squared error (RMSE)
Case 1: all available probe data	Permeability	0.94	13.74	24.09
Case 2: all available probe data	Luminance	0.91	5.69	6.68
Case 3: all available probe data	Porosity (derived from vertical acoustics)	1.00	1.49	1.69
Case 4: all available probe data	Porosity (derived from horizontal acoustics)	1.00	0.67	0.86
Case 5: probe permeability, luminance, horizontal and vertical acoustics	Porosity (derived from vertical acoustics)	0.97	1.70	2.09
Case 6: probe permeability, luminance, horizontal and vertical acoustics	Porosity (derived from horizontal acoustics)	1.00	1.06	1.18

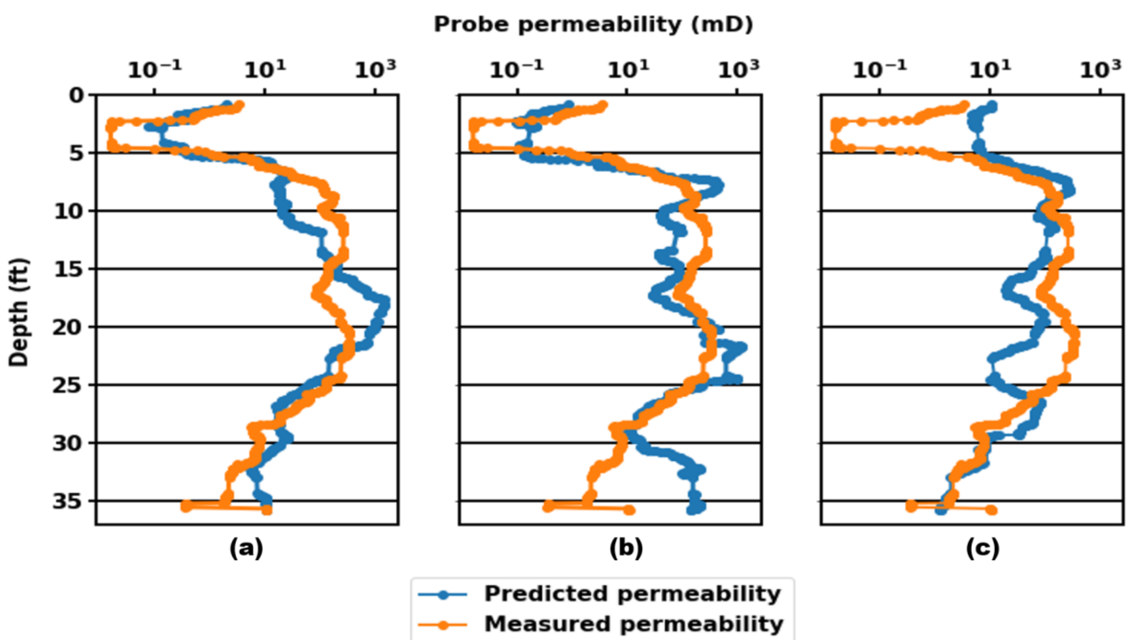

Figure 1: Variation with depth of the smoothed (2 ft vertically averaged) permeability predicted from (a) the luminance, (b) vertical acoustics and (c) horizontal acoustics, along with the smoothed (2 ft vertically averaged) measured probe permeability.

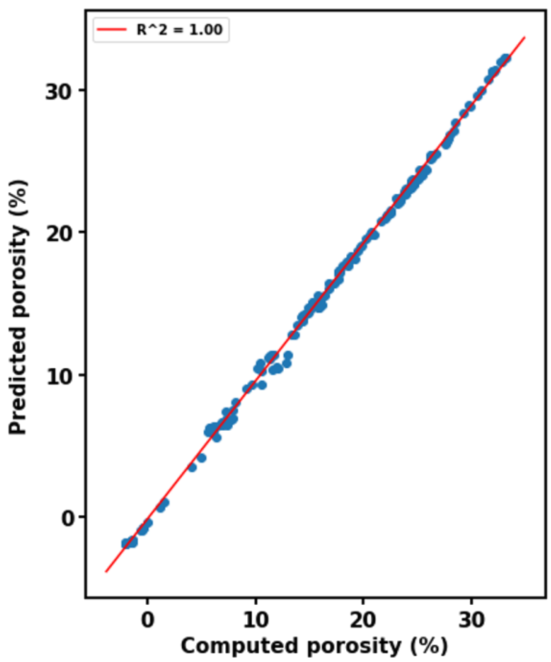

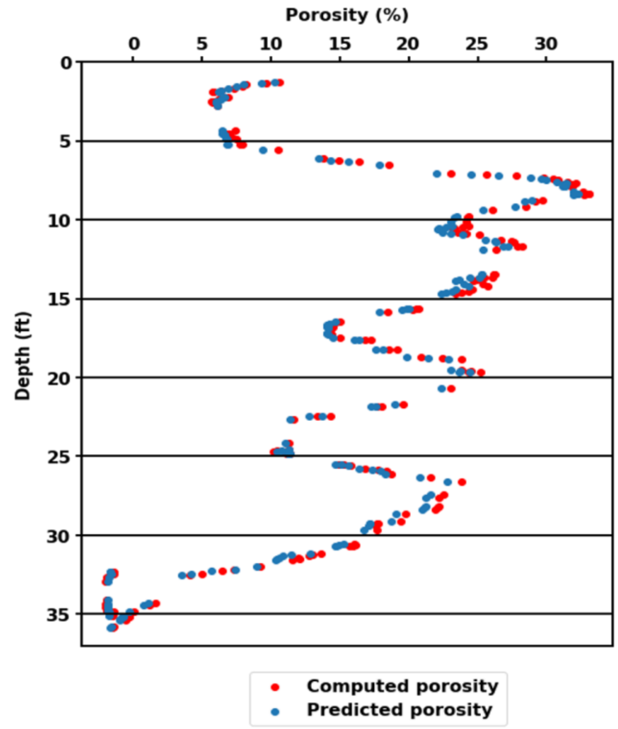

Figure 2: (a) Crossplot of computed porosity (derived from the horizontal probe acoustic data in conjunction with some calibration porosity measurements) and the neural network predicted porosity trained using all the smoothed probe data. **(b)** Variation with depth of computed porosity and the neural network predicted porosity trained using all the smoothed probe data.

References

Osborne, D. A., 1992, Neural Networks Provide More Accurate Reservoir Permeability. *Oil Gas,* vol. 28 (September): p. 80-83.

Sbiga, H. M., and Potter, D. K., 2017, Prediction of resistivity index by use of neural networks with different combinations of wireline logs and minimal core data. *SPE Reservoir Eval. Eng.,* vol. 20 no. 1, p. 240–250. https://doi.org/10.2118/181751-PA

Zhong, Z., Carr, T. R., Wu, X., Wang, G., 2019, Application of a convolutional neural network in permeability prediction: a case study in the Jacksonburg-Stringtown oil field, West Virginia, USA. *Geophysics,* vol. 84, no. 6, p. B363–B373. https://doi.org/10.1190/geo2018-0588.1